

Studying the Galactic Bulge Through Spectroscopy of Microlensed Sources: I. Theoretical Considerations

Stephen R. Kane¹ and Kailash C. Sahu

Space Telescope Science Institute, 3700 San Martin Drive, Baltimore, MD 21218, U.S.A.

skane@stsci.edu, ksahu@stsci.edu

ABSTRACT

The observed spectra of the microlensed sources towards the Galactic bulge may be used as a tool for studying the kinematics and extinction effects in the Galactic bulge. In this paper, we first investigate the expected distribution of the microlensed sources as a function of depth within the Galactic bulge. Our analysis takes a magnitude limited microlensing survey into account, and includes the effects of extinction. We show that, in the current magnitude limited surveys, the probability that the source lies at the far side of the bulge is larger than the probability that the source lies at the near side by a factor of about 2–4. We then investigate the effects of extinction on the observed spectra of microlensed sources. Kurucz model spectra and the observed extinctions towards the Galactic bulge have been used to demonstrate that the microlensed sources should clearly show the effects of extinction which, in turn, can be used as a statistical measure of the contribution of the disk lenses and bulge lenses at different depths. The spectra of the microlensed sources provide a unique probe to derive the radial velocities of a sample which lies preferentially at the far side of the Galactic bulge. The radial velocities, coupled with the microlensing time scales, can thus be useful in studying the 3-dimensional kinematics of the Galactic bulge.

Subject headings: Galaxy: structure — Galaxy: stellar content — stars: kinematics

1. INTRODUCTION

The topic of gravitational microlensing has experienced a dramatic increase in scientific interest over recent years. This has been largely due to the realization of its wide-ranging applications, such as the detection of planets and the study of Galactic structure. More than 400 microlensing events have now been detected toward the Galactic bulge and Magellanic Clouds by the microlensing survey teams EROS, MACHO, OGLE, DUO, and MOA. The contribution of the bulge stars to the

¹Currently at the School of Mathematics and Physics, University of Tasmania, GPO Box 252-21, Hobart, TAS 7001, Australia

observed microlensing optical depth towards the Galactic bulge was estimated to be approximately 60%, the other 40% being due to the stars in the Galactic disk (Kiraga & Paczyński 1994). The optical depth to gravitational microlensing, as estimated from the observed microlensing events by OGLE (Udalski et al. 1994) and MACHO (Alcock et al. 1997), is significantly larger than the values predicted by theoretical models (Paczynski 1991). It has been argued (Paczynski et al. 1994) that the observed optical depth can be best explained if the effect of the Galactic bar and its inclination are correctly taken into account. A consequence of the fact that a large fraction of the events are due to bulge-bulge lensing is, as we will show in more detail later, that the lensed stars will preferentially be located on the far side of the bulge in order that there be sufficient stars along the line of sight to cause microlensing. It was suggested by Stanek (1995) that this would mean that there should be a systematic offset in the apparent magnitude between observed stars and lensed stars. We present a similar discussion by examining the model spectra of different spectral classes and investigating the effects of extinction on stars located on the far side of the bulge.

We first calculate the contributions of the different layers in the bulge to the microlensing optical depth, as has previously been calculated by Kiraga & Paczyński (1994) and Zhao et al. (1995). We have, however, considered the additional effect of extinction in some detail. We then proceed with a discussion on how the spectra of the microlensed sources can be used as a measure of the extinction which, in turn, can be used as a statistical measure of the contribution of the disk lenses and bulge lenses at different depths. We show that the spectra of the microlensed sources can be a useful probe for the 3-dimensional structure of the Galactic bulge. We have also undertaken such a spectroscopic study of the microlensed sources, the details of which will be the subject of a subsequent paper (Kane & Sahu 2000).

2. CALCULATING THE PROBABILITY OF MICROLENSING

The aim here is to calculate the microlensing probability for sources at various depths within the Galactic bulge and to see how the microlensing optical depth varies for sources at various depths taking the effect of extinction into account. For these calculations, the formalism used by Sahu (Sahu 1994a,b) shall be adopted.

Firstly, the number of sources observed at various depths shall be estimated. One of the effects of extinction is the reduction of the observed number of stars at larger depths in the Galactic bulge. Extinction and the distance modulus increase as one goes deeper into the bulge, and both these effects make the sources fainter. So, in a magnitude limited survey (such as the current ones), the observed stellar density decreases as we go from the nearest to the farthest region in a line of sight. Let the ratio of observed stellar number density in the nearest and the farthest region in a given line of sight due to this effect be x .

Let N_{tot} be the number of stars being monitored in a region. For the analysis presented here, it will be assumed that *all* the sources are located within the Galactic bulge. Assuming the extinction

to be uniform in depth, the number of observed stars at any layer dz , at a depth of z (as measured from the observer), may be expressed as

$$N_{obs}(z) = N_z x^{-z/d} \quad (1)$$

where N_z is the observed number of stars per unit depth in the absence of extinction and d is the physical depth of the region being monitored. Integrating this expression yields

$$N_{tot} = \int_0^d N_z x^{-z/d} dz = N_z d \left(\frac{1 - 1/x}{\ln x} \right) \quad (2)$$

Substituting equation (2) into equation (1) gives the following

$$N_{obs}(z) = \frac{N_{tot}}{d} \left(\frac{\ln x}{1 - 1/x} \right) x^{-z/d} \quad (3)$$

The fraction of area covered by the Einstein rings of all the individual stars lying in front of a source at distance D_s may be expressed as

$$A_f(D_s) = \int_0^{D_s} \pi R_E^2(D_d) n(D_d) dD_d \quad (4)$$

where D_d is the distance to the lens and $n(D_d)$ is the stellar number density at distance D_d . If we define $\rho(D_d)$ as the average mass density at depth D_d then we see that $n(D_d) = \rho(D_d)/M$. Since the Einstein ring radius for a lens of mass M in this case is given by

$$R_E = \sqrt{\frac{4GM}{c^2} \frac{D_d(D_s - D_d)}{D_s}} \quad (5)$$

Equation (4) can be rewritten as

$$A_f(D_s) = \frac{4\pi G}{c^2} \int_0^{D_s} \rho(D_d) \frac{D_d(D_s - D_d)}{D_s} dD_d \quad (6)$$

The instantaneous probability that an observed star at a given distance D_s is microlensed, can be written as

$$p = \frac{A_f(D_s) N_{obs}(D_s)}{N_{tot}} \quad (7)$$

The total microlensing optical depth τ can now be calculated. If N_{tot} stars within the bulge are being monitored, then the instantaneous probability of observing a lensing event with an amplification of $A > 1.34$ is given by

$$P = \int_0^d N_{obs}(D_s) A_f(D_s) dD_s \quad (8)$$

The optical depth for microlensing can be written as

$$\tau = P/N_{tot} \quad (9)$$

We will carry out these calculations using 3 different approximations: (i) constant density of stars between the observer and the source, (ii) constant (but different) densities for the disk and the bulge, and (iii) an exponential density model for the bulge. The last approximation is likely to be the best model, and hence the results of this model will be used in our forthcoming spectral analysis (Kane & Sahu 2000). For completeness however, we present the calculations in the other two approximations, since these calculations may be useful for other lines of sight, including the lines of sight far from the Galactic Center, and possibly towards the LMC and M31.

2.1. Constant Density Between Observer and Source

First, let us assume a constant density of matter between the observer and the source and make the substitution $y = D_d/D_s$ then equation (6) becomes

$$\begin{aligned} A_f(D_s) &= \frac{4\pi G D_s^2}{c^2} \int_0^1 \rho(D_d) y(1-y) dy \\ &= \frac{2\pi G \rho D_s^2}{3c^2} \end{aligned} \quad (10)$$

Substituting equation (10) and equation (3) into equation (7) yields

$$p = \frac{2\pi G \rho D_s^2}{3c^2 d} \left(\frac{\ln x}{1 - 1/x} \right) x^{-D_s/d} \quad (11)$$

This probability p is plotted in Figure 1 as a function of D_s assuming a density of $\rho = 0.20 M_\odot \text{pc}^{-3}$.

As seen in Figure 1, in the case of zero extinction the fractional area covered by the Einstein rings of the lenses increases dramatically with distance. However, the number of observed stars decreases with distance if there is internal extinction. As seen in equation (7), the probability is a multiplication of these two functions which, as demonstrated in Figure 1, is dominated by the first effect for a reasonable value of extinction. Table 1 shows the difference in probability of microlensing for stars located at a distance of $D_s = 7.0 \text{ kpc}$ and stars located at a distance of $D_s = 9.0 \text{ kpc}$.

Substituting equation (3) and equation (10) into equation (8) gives

$$P = \frac{2\pi G \rho}{3c^2} \frac{N_{tot}}{d} \left(\frac{\ln x}{1 - 1/x} \right) \int_0^d x^{-D_s/d} D_s^2 dD_s \quad (12)$$

where the integrand can be solved analytically via repeated integration by parts. Dividing the result by N_{tot} yields an expression for the optical depth for gravitational microlensing

$$\tau = \frac{2\pi G \rho d^2}{3c^2} \frac{x}{x-1} \left(\frac{2}{(\ln x)^2} - \frac{1}{x} - \frac{2}{x \ln x} - \frac{2}{x(\ln x)^2} \right) \quad (13)$$

The value of τ as given in equation (13) is plotted in Figure 2 as a function of x , which shows the variation of optical depth with increasing extinction.

However, the assumption of constant density along the line of sight may be valid for microlensed sources in the Galactic disk (e.g., OGLE-1999-CAR-01 (Udalski et al. 2000)), but can not be applied to sources in the Galactic bulge.

2.2. Constant Density for Disk and Bulge

If a constant density of matter for the disk ρ_d and for the bulge ρ_b is assumed (see Figure 3), equation (6) becomes

$$A_f(D_s) = \frac{4\pi G}{c^2} \left(\int_0^b \rho_d \frac{D_d(D_s - D_d)}{D_s} dD_d + \int_b^{D_s} \rho_b \frac{D_d(D_s - D_d)}{D_s} dD_d \right) \quad (14)$$

where b is the distance from the observer to the near side of the bulge. Since the optical depth of microlensing of disk stars is relatively small (Kiraga & Paczyński 1994), we have assumed that all the sources are within the Galactic bulge, i.e., $D_s > b$.

Making the substitution $y = D_d/D_s$, equation (14) simplifies to

$$A_f(D_s) = \frac{4\pi G D_s^2}{c^2} \left(\rho_d \int_0^{b/D_s} y(1-y) dy + \rho_b \int_{b/D_s}^1 y(1-y) dy \right) \quad (15)$$

Solving this yields the following expression for the fractional area covered by the Einstein rings, which is the same as the probability that a given star at a distance D_s is microlensed at any given time:

$$A_f(D_s) = \frac{4\pi G}{c^2} \left(\rho_d \left(\frac{b^2}{2} - \frac{b^3}{3D_s} \right) + \rho_b \left(\frac{D_s^2}{6} - \frac{b^2}{2} + \frac{b^3}{3D_s} \right) \right) \quad (16)$$

The first term is the contribution of the disk lenses and the second term is that of the bulge lenses.

Let $b = 7.0 \text{ kpc}$, $d = 9.0 \text{ kpc}$, $\rho_d = 0.07 M_\odot \text{ pc}^{-3}$, and $\rho_b = 0.50 M_\odot \text{ pc}^{-3}$. Substituting equation (16) and equation (3) into equation (7) yields the instantaneous probability that an observed star at a given distance D_s is microlensed

$$p = \frac{4\pi G}{c^2(d-b)} \left(\frac{\ln x}{1-1/x} \right) x^{-\frac{D_s-b}{d-b}} \left(\rho_d \left(\frac{b^2}{2} - \frac{b^3}{3D_s} \right) + \rho_b \left(\frac{D_s^2}{6} - \frac{b^2}{2} + \frac{b^3}{3D_s} \right) \right) \quad (17)$$

This probability p is plotted in Figure 4 as a function of D_s using the above parameters for the bulge.

Figure 4 shows that, when a constant density is assumed for the bulge, the probability of sources on the far side of the bulge being microlensed quickly becomes dominated by the level of extinction. Indeed the stars located at the near side of the bulge ($D_s = 7.0 \text{ kpc}$) have a larger

probability of being microlensed than those located at the far side of the bulge ($D_s = 9.0$ kpc) for $x \gtrsim 2$, as shown in Table 2.

For completeness, the total microlensing optical depth will now be calculated. Substituting equation (3) and equation (16) into equation (8) and dividing by N_{tot} yields an expression for the optical depth for gravitational microlensing

$$\tau = \frac{4\pi G}{c^2(d-b)} \left(\frac{\ln x}{1-1/x} \right) \int_b^d \left((\rho_b - \rho_d) x^{-\frac{D_s-b}{d-b}} \left(\frac{b^3}{3D_s} - \frac{b^2}{2} \right) + \frac{\rho_b}{6} x^{-\frac{D_s-b}{d-b}} D_s^2 \right) dD_s \quad (18)$$

The value of τ as given in equation (18) is plotted in Figure 5 as a function of x , which shows the variation of optical depth with increasing extinction. For $x = 3.0$ the optical depth is $\approx 5.57 \times 10^{-7}$ and for $x = 7.0$ the optical depth is $\approx 5.17 \times 10^{-7}$. These values are only slightly lower than an optical depth of $\approx 8.5 \times 10^{-7}$ estimated by Kiraga & Paczyński (1994) using a similar Galactic model but without taking extinction into account. This is the result one would expect when extinction is added to the optical depth calculations. However, this calculation is dependent upon the choice of ρ_d and ρ_b which, given the nature of the model, will be crude estimates at best.

2.3. Exponential Density Model for Bulge

An even better approximation of the distribution of matter between the observer and the source is to use an exponential-type function to represent the density profile over the Galactic bulge. The model used to do this is a simplified version of the E2 triaxial Galactic bulge model fitted by Dwek et al. (1995) with an exponential cutoff at 2.4 kpc. This model is defined as

$$\rho_{E2}(i, j, k) = \rho_0 \exp(-r) \quad (19)$$

where

$$r = \left[\left(\frac{i}{i_0} \right)^2 + \left(\frac{j}{j_0} \right)^2 + \left(\frac{k}{k_0} \right)^2 \right]^{1/2} \quad (20)$$

is the distance from the Galactic centre. Treating this from a purely radial perspective and centering the coordinate system on the observer results in the density profile given by

$$\rho(D_d) = \rho_0 \exp \left[-\frac{|R_0 - D_d|}{i_0} \right] \quad (21)$$

where the normalisation constant is given by

$$\rho_0 = \frac{M}{8\pi i_0 j_0 k_0} \quad (22)$$

The value of ρ_0 shall be calculated by adopting the total bulge mass estimated by Dwek et al. (1995) of $M = 1.3 \times 10^{10} M_\odot$ and using the scale lengths of $i_0 = 0.71$, $j_0 = 0.18$, and $k_0 = 0.25$ kpc

for a Galactocentric distance of $R_0 = 8.0$ kpc. This model is valid for a line of sight that passes approximately through the Galactic center.

Using this model, equation (6) becomes

$$A_f(D_s) = \frac{4\pi G\rho_0}{c^2} \int_0^{D_s} \exp\left[-\frac{|R_0 - D_d|}{i_0}\right] \frac{D_d(D_s - D_d)}{D_s} dD_d \quad (23)$$

Solving this equation (see Appendix) yields the following expression for the fractional area covered by the Einstein rings:

$$A_f(D_s) = \begin{cases} \frac{4\pi G\rho_0}{c^2} \frac{i_0^2 e^{-R_0/i_0} \alpha}{D_s} & \text{for } D_s < R_0 \\ \frac{4\pi G\rho_0}{c^2} \frac{i_0(2i_0^2\beta - 2R_0^2 + D_s\gamma)}{D_s} & \text{for } D_s > R_0 \end{cases} \quad (24)$$

where

$$\begin{aligned} \alpha &= D_s(1 + e^{D_s/i_0}) + 2i_0(1 - e^{D_s/i_0}) \\ \beta &= e^{-(D_s - R_0)/i_0} + e^{-R_0/i_0} - 2 \\ \gamma &= i_0 e^{-(D_s - R_0)/i_0} + i_0 e^{-R_0/i_0} + 2R_0 \end{aligned}$$

Substituting equation (24) and equation (3) into equation (7) yields the instantaneous probability that an observed star at a given distance D_s is microlensed

$$p = \begin{cases} \frac{4\pi G\rho_0}{c^2(d-b)} \left(\frac{\ln x}{1-1/x}\right) x^{-\frac{D_s-b}{d-b}} \left(\frac{i_0^2 e^{-R_0/i_0} \alpha}{D_s}\right) & \text{for } D_s < R_0 \\ \frac{4\pi G\rho_0}{c^2(d-b)} \left(\frac{\ln x}{1-1/x}\right) x^{-\frac{D_s-b}{d-b}} \left(\frac{i_0(2i_0^2\beta - 2R_0^2 + D_s\gamma)}{D_s}\right) & \text{for } D_s > R_0 \end{cases} \quad (25)$$

where we have assumed that all the sources are within the Galactic bulge, i.e., $D_s > b$. This probability p is plotted in Figure 6 as a function of D_s using the above model.

Figure 6 shows that an exponential density model dramatically increases the domination of the fractional area in the probability of microlensing. For stars located at the far side of the bulge ($D_s = 9.0$ kpc) the probability of being microlensed is significantly larger than those located at the near side of the bulge ($D_s = 7.0$ kpc), as shown in Table 3.

The total microlensing optical depth can now be calculated. Substituting Equation (3) and Equation (24) into Equation (8) and dividing by N_{tot} yields an expression for the optical depth for gravitational microlensing

$$\tau = \begin{cases} \frac{4\pi G\rho_0}{c^2(d-b)} \left(\frac{\ln x}{1-1/x}\right) i_0^2 e^{-R_0/i_0} \int_b^d x^{-\frac{D_s-b}{d-b}} \frac{\alpha}{D_s} dD_s & \text{for } D_s < R_0 \\ \frac{4\pi G\rho_0}{c^2(d-b)} \left(\frac{\ln x}{1-1/x}\right) i_0 \int_b^d x^{-\frac{D_s-b}{d-b}} \frac{2i_0^2\beta - 2R_0^2 + D_s\gamma}{D_s} dD_s & \text{for } D_s > R_0 \end{cases} \quad (26)$$

The value of τ as given in Equation (26) is plotted in Figure 7 as a function of x , which shows the variation of optical depth with increasing extinction. For $x = 3.0$ the optical depth is $\approx 3.53 \times 10^{-6}$

and for $x = 7.0$ the optical depth is $\approx 2.77 \times 10^{-6}$. These estimates for the microlensing optical depth towards the Galactic bulge are close to the values of $(3.3 \pm 1.2) \times 10^{-6}$ and $(3.9_{-1.2}^{+1.8}) \times 10^{-6}$ measured by Udalski et al. (1994) and Alcock et al. (1997) respectively. Alcock et al. (2000a) derive a value of $\tau_{total} = (2.43_{-0.38}^{+0.39}) \times 10^{-6}$ from difference image analysis, and Popowski et al. (2000) derive a value of $\tau = (2.43 \pm 0.4) \times 10^{-6}$, which are also consistent with our estimated value. Zhao et al. (1995) and Paczyński et al. (1994) have estimated a similar value of $(2.2 \pm 0.45) \times 10^{-6}$ and $(3.3 \pm 1.2) \times 10^{-6}$, respectively, by taking the inclination of the bar into account.

The limiting apparent magnitude of the current surveys is about $m_V = 20$ which at the near side of the bulge would correspond to an absolute magnitude of $M_V = 5.8$ and an absolute magnitude of $M_V = 5.3$ at the far side of the bulge were there no extinction. However, the estimated foreground extinction towards Baade’s window has been estimated by Stanek (1996) to lie in the range of 1.26 to 2.79 magnitudes, depending on the line of sight. Hence the limiting absolute magnitudes of the stars in this direction lies in the range $M_V = 4.5$ to 2.5 (including the 0.5 magnitudes because of the larger distance). If the distribution of stars amongst different spectral types is assumed to be similar to what is observed in the solar neighbourhood (Kroupa et al. 1993; Weilen et al. 1983) then the stellar number density is relatively flat in this region. This distribution shows that the ratio in the observed stellar number density from the near to far side of the bulge is between ~ 2.6 to 5.3, depending on the internal extinction.

For $x = 3.0$ the fractional area at the far side of the bulge is ≈ 4.2 times that at the near side of the bulge. For $x = 5.0$ the fractional area at the far side of the bulge is ≈ 2.5 times that at the near side of the bulge. This means that, on average, stars that are lensed in Baade’s window are about 2–4 times more likely to be at the far side of the bulge than the near side.

If lensed stars are indeed predominantly on the far side of the bulge then this provides us with a useful tool for studying the Galactic structure at the far side of the bulge. Radial velocity measurements from spectra of microlensed sources combined with the measured time scale of the events may be used as a unique probe into the 3-dimensional kinematics of the far side of the bulge.

2.4. Effect of the Galactic Bar

We have so far neglected the effect of the Galactic bar. The Galactic bar, however, is known to exist both from infrared and microlensing observations (Gerhard 2000; Hammersley et al. 2000; Paczyński et al. 1994). A number of photometric and dynamic indications also point out the presence of the Galactic bar (Binney et al. 1991; Whitelock et al. 1991; Weinberg 1992). The effect of the bar is not only obvious from the microlensing observations, but its inclination might be essential to account for the optical depth observed in at least some of the lines of sight (also see Binney et al. (2000)). Furthermore, the inclination of the major axis of the bar with respect to the line of sight, as independently determined from the microlensing observations, is consistent with the inclination of ~ 15 degrees determined from the earlier infrared observations. So a natural

question to ask is, how does the presence of the Galactic bar effect the analysis presented here? In particular, what is the effect of the Galactic bar on the spectroscopic observations, both in terms of extinction and kinematics?

The effect of the Galactic bar is expected to be seen even more clearly in the spectroscopic observations. The reason is two-fold. The first part has to do with the extinction. A good part of the Baade’s window is thought to have little extinction. The Galactic bar on the other hand, which clearly occupies only a part of the region surveyed for microlensing (cf. Alcock et al. (1997); Udalski et al. (1994); Blitz & Spergel (1991)), is bright in the far-infrared wavelengths as seen in the IRAS SKYFLUX maps (Beichman et al. 1985), clearly indicating the presence of cool dust. In such a case, the microlensed sources in the region of the Galactic bar should certainly show larger extinction compared to the unlensed sources. The second part has to do with the expected kinematics. Although there is some uncertainty in the models, the objects in the Galactic bar, in general, are expected to be kinematically distinct from those in the outer parts of the bulge (see, for example, Blitz & Spergel (1991); Kent (1987)). Thus the effect of the bar may be more prominently seen in the kinematic distribution. Indeed, the kinematics of the microlensed sources may provide very meaningful constraints on the structure of the bar. In order to see this extra effect of the Galactic bar, however, the observations must be done for the sources in a restricted region covering the Galactic bar.

2.5. Blending Effects

The Galactic bulge fields are crowded in general. As a result, many of the microlensed sources may be blended with other stars, and this effect must be taken into account in estimating the extinctions and the radial velocities of the microlensed sources from the observed spectra. (Note that the blending has no effect on the theoretical estimate of the optical depth described above. The discussion here refers only to the spectroscopic observations and role of blending in such observations). As the recent HST images towards the LMC and the Galactic bulge show, blending can be an important effect. In the case of the microlensing events towards the LMC, each ‘microlensed star’ typically splits into 2 or more sources in the high spatial-resolution HST image (Alcock et al. 2000b). Towards the Galactic bulge, however, for which the distance is about 7 times smaller than the LMC, blending may be less severe.

The effect of blending is discussed in detail by Di Stefano & Esin (1995), including the effects of blending when inferring properties of underlying populations through the statistical study of lensing events (Dominik & Sahu 2000; Woźniak & Paczyński 1997). The effect of blending can be summarized as follows: (i) Blending makes it more difficult to observe a microlensing event since the observed amplification is smaller than the actual amplification. This decreases the efficiency of the detection of a microlensing event. (ii) Blending enables some stars which are otherwise invisible in the sample to be included in the sample of the monitored events. This increases the efficiency of detection. (iii) The effect of blending is to increase the number of monitored stars, thus increasing

the net efficiency of detection.

The first effect tends to offset the latter two. The net effect depends on the brightness of the source/lens, and the crowding of the field. So far as our analysis of extinction is concerned, since the blending star is expected to be preferentially closer than the microlensed source, blending dilutes the effect of extinction. As Di Stefano & Esin (1995) point out, the effect of blending is more important for fainter sources. A full analysis of blending is beyond the scope of this work. However, our preliminary estimate suggests that, if the microlensed star is brighter than $m_V \sim 18$, the contribution of the blended star is about 10%. This contribution increases to more than 50% for stars with $m_V \sim 20$. Thus, if the analysis is confined to brighter sources (as is the case for the sources presented in Kane & Sahu (2000)), the effect of blending can be neglected in the analysis of the spectroscopic observations.

3. EFFECTS OF EXTINCTION ON SPECTRA

It has been shown that a predominant fraction of microlensed sources are located on the far side of the Galactic bulge. This can be observationally confirmed by observing the extinction effects in the spectra of the lensed stars which, in turn, can be used to estimate the fractional contributions of the disk and bulge stars to the total microlensing optical depth.

To simulate the effects of extinction on various spectral types, the spectral models used were those from the Kurucz database (Dr. R. Kurucz, CD-ROM No. 13 (Kurucz 1993)). Each of the Kurucz models used have been normalized for a solar metallicity and a distance of $D_s = 9.0$ kpc. Each of the model spectra are recalculated for E_{B-V} values of 0.0, 0.2, 0.4, 0.6, 0.8 where the extinction corrected spectrum, s_c , is calculated from the raw spectrum, s_r , via

$$(s_c)_\lambda = (s_r)_\lambda \times 10^{-(E_{B-V} \times e_g)/2.5} \quad (27)$$

where

$$e_g = \frac{A_\lambda}{E_{B-V}} \quad (28)$$

The data for the Galactic extinction, e_g , was taken from Seaton (1979).

Table 4 shows the stellar parameters used for the model spectra, where T_{eff} is the effective temperature, $\log g$ is the log gravity, and m_V is the apparent magnitude of the star. Then varying E_{B-V} from 0.4 to 0.8 is fairly representative of the levels of extinction that exist within Baade's window, suggested by Stanek (1996) to be in the range of 1.26 to 2.79 magnitudes.

Figures 8, 9, 10, and 11 show the effect of extinction on observed spectra of various types of stars given in Table 4. There is a significant change in spectral features, such as slope and line strength, from an E_{B-V} value of 0.0 to 0.8. The slope and the features can be used to quantitatively estimate the extinction of the microlensed stars in comparison to the general sample in the Galactic bulge. It is apparent from the model spectra that, although blue stars in the main sequence will

always be brighter than red main-sequence stars at all wavelengths, the effects of extinction will cause the stellar population at the far side of the bulge to discriminate against blue stars as source stars in microlensing.

From our previous arguments, we expect a majority of the microlensed sources to show an extinction value between $E_{B-V} = 0.4$ and $E_{B-V} = 0.8$. Clearly, a collection of microlensed source spectra bearing this characteristic would become statistically significant when estimating the contribution of bulge-bulge lensing to the microlensing optical depth. If this is shown to be statistically the case then this simple method can be used as a statistical distance indicator for microlensed sources.

A knowledge of the distance to the source enables the distance to the lens to be estimated. To demonstrate this, the Galactic bulge model outlined in Section 1.3 shall be used. For a source located at a distance D_s , the fractional area covered by the Einstein rings of the intervening stars at a depth dD_d at a distance D_d is

$$A_f(D_d) dD_d = \frac{4\pi G}{c^2} \rho_0 \exp \left[-\frac{|R_0 - D_d|}{i_0} \right] \frac{D_d(D_s - D_d)}{D_s} dD_d \quad (29)$$

As discussed earlier, the probability distribution of the distance to the source peaks at 9.0 kpc. The probability distribution of the location of the lenses (in units of the distance to the source) is shown in Figure 12, which shows that the probability peaks at a distance of $D_d = 0.85D_s$ which, for $D_s = 9.0$ kpc, corresponds to $D_d = 7.8$ kpc. It is worth noting that this does not imply that most of the lenses are at $D_d = 7.8$ kpc. This only implies that a lens distance of $0.85 D_s$ is twice more likely than a lens distance of $0.6 D_s$.

Since the angular Einstein ring radius is known from the characteristic time scale of the event, the extinction exhibited in the spectra of microlensed sources can be used as a means to estimate the size of the Einstein ring radius in terms of AU. Detectable deviations in microlensing light curves due to planetary masses depend highly upon the star-planet distance in the lensing system (Bennett & Rhie 1996; Gaudi & Sackett 2000), making this method a useful technique to constrain calculations of planet detection efficiencies.

4. CONCLUSIONS

Various Galactic models have been used to demonstrate the theoretical effects of extinction upon the microlensing optical depth. The exponential density model provides the best approximation of the microlensing optical depth when taking extinction into account. For the exponential model, it is shown that stars that are lensed within Baade’s window are about 2–4 times more likely to be at the far side of the bulge than the near side. The estimated optical depth is $\approx 3.53 \times 10^{-6}$ for $x = 3.0$, which is close to the observed optical depths of $(3.3 \pm 1.2) \times 10^{-6}$ and $(3.9^{+1.8}_{-1.2}) \times 10^{-6}$ measured by Udalski et al. (1994) and Alcock et al. (1997) respectively.

The effects of extinction on spectra of microlensed sources have been simulated using Kurucz model spectra. It is shown that the majority of microlensed sources should exhibit extinction between $E_{B-V} = 0.4$ and $E_{B-V} = 0.8$. It is also shown that using extinction as a distance indicator for microlensed sources may be used to statistically estimate the distance to the lens from the probability distribution corresponding to the appropriate Galactic model.

The measured extinctions for the microlensed sources can be used to determine the expected stellar number density gradient x which, in turn, can be used to determine the optical depth more accurately. If there is a smooth velocity gradient within the Galactic bulge, one would expect a statistical correlation between the radial velocity and the extinction of microlensed sources which, given enough samples, will provide useful information regarding the 3-dimensional velocity structure of the far side of the Galactic bulge. Given the variation in extinction through the Galactic bulge, the sample would require ~ 100 spectra of microlensed sources in order to clearly show the described effects.

The authors would like to thank Dr. Eric Agol for several useful discussions regarding the Galactic bulge model calculations. Thanks are also due to Dr. Rosanne Di Stefano for her useful comments regarding blending.

A. FRACTIONAL AREA FOR EXPONENTIAL DENSITY

This appendix details the evaluation of the integral in equation (23). Let the integral be defined as

$$I = \int_0^{D_s} \exp\left[-\frac{|R_0 - D_d|}{i_0}\right] \frac{D_d(D_s - D_d)}{D_s} dD_d \quad (\text{A1})$$

Due to the absolute value of $R_0 - D_d$, this integral is a boundary value problem around the Galactocentric distance R_0 . Hence, the integral needs to be separated into two integrals defined on either of the boundary R_0 , as follows

$$I_1 = \int_0^{D_s} \exp\left[-\frac{(R_0 - D_d)}{i_0}\right] \frac{D_d(D_s - D_d)}{D_s} dD_d$$

for $D_s < R_0$, and

$$I_2 = \int_0^{R_0} \exp\left[-\frac{(R_0 - D_d)}{i_0}\right] \frac{D_d(D_s - D_d)}{D_s} dD_d + \int_{R_0}^{D_s} \exp\left[-\frac{(D_d - R_0)}{i_0}\right] \frac{D_d(D_s - D_d)}{D_s} dD_d$$

for $D_s > R_0$. These two integrals will now be considered separately.

A.1. Source Distance Less Than R_0

The integral I_1 may be expanded into two parts

$$I_1 = \int_0^{D_s} D_d \exp \left[-\frac{(R_0 - D_d)}{i_0} \right] dD_d - \int_0^{D_s} \frac{D_d^2}{D_s} \exp \left[-\frac{(R_0 - D_d)}{i_0} \right] dD_d \quad (\text{A2})$$

Both of these integrals may be evaluated using integration by parts:

$$\int u \frac{dv}{dx} dx = uv - \int v \frac{du}{dx} dx$$

In the case of the first integral, it is most convenient to define

$$u = D_d \text{ and } \frac{dv}{dD_d} = \exp \left[-\frac{(R_0 - D_d)}{i_0} \right]$$

Then it follows that

$$\frac{du}{D_d} = 1 \text{ and } v = \int \exp \left[-\frac{(R_0 - D_d)}{i_0} \right] D_d$$

By substituting $\gamma = (R_0 - D_d)/i_0$, v becomes

$$\begin{aligned} v &= -i_0 \int e^{-\gamma} d\gamma \\ &= i_0 e^{-\gamma} \\ &= i_0 \exp \left[-\frac{(R_0 - D_d)}{i_0} \right] \end{aligned}$$

Then using integration by parts

$$\begin{aligned} \int u \frac{dv}{dD_d} dD_d &= D_d i_0 \exp \left[-\frac{(R_0 - D_d)}{i_0} \right] - i_0 \int \exp \left[-\frac{(R_0 - D_d)}{i_0} \right] dD_d \\ &= i_0 D_d \exp \left[-\frac{(R_0 - D_d)}{i_0} \right] - i_0^2 \exp \left[-\frac{(R_0 - D_d)}{i_0} \right] \\ &= i_0 \exp \left[-\frac{(R_0 - D_d)}{i_0} \right] (D_d - i_0) \end{aligned} \quad (\text{A3})$$

In the case of the second integral, it is convenient to define

$$u = \frac{D_d^2}{D_s} \text{ and } \frac{dv}{dD_d} = \exp \left[-\frac{(R_0 - D_d)}{i_0} \right]$$

Then it follows that

$$\frac{du}{D_d} = \frac{2D_d}{D_s} \text{ and } v = i_0 \exp \left[-\frac{(R_0 - D_d)}{i_0} \right]$$

Then using integration by parts

$$\begin{aligned}
\int u \frac{dv}{dD_d} dD_d &= \frac{D_d^2}{D_s} i_0 \exp\left[-\frac{(R_0 - D_d)}{i_0}\right] - \frac{2i_0}{D_s} \int D_d \exp\left[-\frac{(R_0 - D_d)}{i_0}\right] dD_d \\
&= i_0 \frac{D_d^2}{D_s} \exp\left[-\frac{(R_0 - D_d)}{i_0}\right] - \frac{2i_0^2}{D_s} \exp\left[-\frac{(R_0 - D_d)}{i_0}\right] (D_d - i_0) \\
&= \frac{i_0}{D_s} \exp\left[-\frac{(R_0 - D_d)}{i_0}\right] (D_d^2 - 2i_0 D_d + 2i_0^2)
\end{aligned} \tag{A4}$$

Combining Equation A.3 and Equation A.4 yields

$$I_1 = i_0 \exp\left[-\frac{(R_0 - D_d)}{i_0}\right] \left(D_d - i_0 - \frac{D_d^2}{D_s} + \frac{2i_0 D_d}{D_s} - \frac{2i_0^2}{D_s}\right) \Big|_{D_d=0}^{D_d=D_s} \tag{A5}$$

$$\begin{aligned}
&= i_0^2 \exp\left[-\frac{(R_0 - D_s)}{i_0}\right] \left(1 - \frac{2i_0}{D_s}\right) + i_0^2 \exp\left[-\frac{R_0}{i_0}\right] \left(1 + \frac{2i_0}{D_s}\right) \\
&= \frac{i_0^2 e^{-R_0/i_0} (D_s(1 + e^{D_s/i_0}) + 2i_0(1 - e^{D_s/i_0}))}{D_s}
\end{aligned} \tag{A6}$$

A.2. Source Distance Greater Than R_0

Since the first component of integral I_2 is identical to integral I_1 except for the limits, this component may be solved by simply substituting the limits $0 \rightarrow R_0$ into Equation A.5.

$$\begin{aligned}
I_{2.1} &= i_0 \exp\left[-\frac{(R_0 - D_d)}{i_0}\right] \left(D_d - i_0 - \frac{D_d^2}{D_s} + \frac{2i_0 D_d}{D_s} - \frac{2i_0^2}{D_s}\right) \Big|_{D_d=0}^{D_d=R_0} \\
&= i_0 \left(R_0 - i_0 - \frac{R_0^2}{D_s} + \frac{2i_0 R_0}{D_s} - \frac{2i_0^2}{D_s}\right) - i_0 \exp\left[-\frac{R_0}{i_0}\right] \left(-i_0 - \frac{2i_0^2}{D_s}\right) \\
&= \frac{i_0(R_0 D_s + 2i_0 R_0 + i_0 e^{-R_0/i_0} (D_s + 2i_0) - i_0 D_s - 2i_0^2 - R_0^2)}{D_s}
\end{aligned} \tag{A7}$$

As was the case for integral I_1 , the second component of integral I_2 may be solved by expanding the integral into two parts

$$I_{2.2} = \int_{R_0}^{D_s} D_d \exp\left[-\frac{(D_d - R_0)}{i_0}\right] dD_d - \int_{R_0}^{D_s} \frac{D_d^2}{D_s} \exp\left[-\frac{(D_d - R_0)}{i_0}\right] dD_d$$

Using integration by parts, the first integral becomes

$$I_{2.2.1} = -i_0 \exp\left[-\frac{(D_d - R_0)}{i_0}\right] (D_d + i_0) \tag{A8}$$

and the second integral becomes

$$I_{2.2.2} = -\frac{i_0}{D_s} \exp\left[-\frac{(D_d - R_0)}{i_0}\right] (D_d^2 + 2i_0 D_d + 2i_0^2) \tag{A9}$$

so that combining Equation A.8 and Equation A.9 yields

$$\begin{aligned}
 I_{2.2} &= i_0 \exp \left[-\frac{(D_d - R_0)}{i_0} \right] \left(-D_d - i_0 + \frac{D_d^2}{D_s} + \frac{2i_0 D_d}{D_s} + \frac{2i_0^2}{D_s} \right) \Big|_{D_d=R_0}^{D_d=D_s} \\
 &= i_0 \exp \left[-\frac{(D_s - R_0)}{i_0} \right] \left(i_0 + \frac{2i_0^2}{D_s} \right) - i_0 \left(-R_0 - i_0 + \frac{R_0^2}{D_s} + \frac{2i_0 R_0}{D_s} + \frac{2i_0^2}{D_s} \right) \\
 &= \frac{i_0(i_0 D_s - 2i_0^2 + i_0 e^{-(D_s - R_0)/i_0} (D_s + 2i_0) + R_0 D_s - 2i_0 R_0 - R_0^2)}{D_s}
 \end{aligned} \tag{A10}$$

Combining Equation A.7 and Equation A.10 leads to the expression for integral I_2

$$I_2 = \frac{i_0 \left(2i_0^2 \left(e^{-\frac{D_s - R_0}{i_0}} + e^{-\frac{R_0}{i_0}} - 2 \right) - 2R_0^2 + D_s \left(i_0 e^{-\frac{D_s - R_0}{i_0}} + i_0 e^{-\frac{R_0}{i_0}} + 2R_0 \right) \right)}{D_s} \tag{A11}$$

REFERENCES

- Alcock, C., et al. 1997, ApJ, 479, 119
- Alcock, C., et al. 2000, ApJ, 541, 734
- Alcock, C., et al. 2000, in press (astro-ph/0008282)
- Bennett, D.P. & Rhie, S.H. 1996, ApJ, 472, 660
- Beichman, C.A., Neugebauer, G., Habing, H.J., Clegg, P.E. & Chester, T.J., 1985, *IRAS Explanatory Supplement*, published by JPL, Pasadena
- Binney, J. J., Gerhard, O. E., Stark, A. A., Bally, J., & Uchida, K. I. 1991, MNRAS, 252, 210
- Binney, J., Bissantz, N. & Ortwin, G., 2000, ApJ, 537, L99
- Blitz, L. & Spergel, D. 1991, ApJ, 379, 631
- Di Stefano, R. & Esin, A.A. 1995, ApJ, 448, L1
- Dominik, M. & Sahu, K.C. 2000, ApJ, 534, 213
- Dwek, E., et al. 1995, ApJ, 445, 716
- Gaudi, B.S. & Sackett, P.D. 2000, ApJ, 528, 56
- Gerhard, O. 2000, in *Disk Galaxies and Galaxy Disks*, ASP Conf. Ser., in press, (astro-ph/0010539)
- Hammersley, P.L., Garzon, F., Mahoney, T.J., Lopez-Corredoira, M., Torres, M.A.P., 2000, MNRAS, 317, L45

- Kane, S.R. & Sahu K.C. 2000, in preparation
- Kent, S. 1987, AJ, 93, 1062
- Kiraga, M. & Paczyński, B. 1994, ApJ, 430, L101
- Kroupa, P., Tout, C.A., & Gilmore, G. 1993, MNRAS, 262, 545
- Kurucz, R. 1993, ATLAS9 Stellar Atmosphere Programs and 2 km/s grid. Kurucz CD-ROM No. 13. Cambridge, MA: Smithsonian Astrophysical Observatory
- Paczynski, B. 1991, ApJ, 371, L63
- Paczynski, B., et al. 1994, ApJ, 435, L113
- Popowski, P., et al. 2000, in *Microlensing 2000: A New Era of Microlensing Astrophysics*, ASP Conf. Ser. Ed. J.W. Menzies and P.D.Sackett, in press (astro-ph/0005466)
- Sahu, K.C. 1994a, PASP, 106, 942
- Sahu, K.C. 1994b, Nature, 370, 275
- Seaton, M.J. 1979, MNRAS, 187, 73p
- Stanek, K.Z. 1995, ApJ, 441, L29
- Stanek, K.Z. 1996, ApJ, 460, L37
- Udalski, A., et al. 1994, Acta Astronomica, 44, 165
- Udalski, A., et al. 2000, Acta Astronomica, 50, 1
- Weilen, R., Jahreiss, H., Krüger, R. 1983, in IAU Colloq. 76, The Nearby Stars and the Stellar Luminosity Function, ed. A.G. Davis Philip & A.R. Upgren (Schenectady: Davis), p.163
- Whitelock, P., Feast, M. & Catchpole, R. 1991, MNRAS, 248, 276
- Weinberg, D. 1992, ApJ, 384, 81
- Woźniak, P. & Paczyński, B. 1997, ApJ, 487, 55
- Zhao, H., Spergel, D.N., & Rich, R.M. 1995, ApJ, 440, L13

Table 1. Variation of instantaneous probability of microlensing with extinction x for a constant density between the observer and the source.

x	$A_f(7)N_{obs}(7)/N_{tot}(10^{-8})$	$A_f(9)N_{obs}(9)/N_{tot}(10^{-8})$
1.0	10.92	18.04
2.0	8.83	12.51
3.0	7.66	9.91
4.0	6.87	8.34
5.0	6.28	7.26
6.0	5.83	6.47
7.0	5.46	5.85

Table 2. Variation of instantaneous probability of microlensing with extinction x for a constant density for the disk and bulge.

x	$A_f(7)N_{obs}(7)/N_{tot}(10^{-7})$	$A_f(9)N_{obs}(9)/N_{tot}(10^{-7})$
1.0	1.77	5.12
2.0	2.45	3.55
3.0	2.92	2.81
4.0	3.27	2.36
5.0	3.56	2.06
6.0	3.80	1.83
7.0	4.02	1.66

Table 3. Variation of instantaneous probability of microlensing with extinction x for an exponential density model.

x	$A_f(7)N_{obs}(7)/N_{tot}(10^{-6})$	$A_f(9)N_{obs}(9)/N_{tot}(10^{-6})$
1.0	0.48	6.07
2.0	0.66	4.21
3.0	0.79	3.33
4.0	0.88	2.80
5.0	0.96	2.44
6.0	1.03	2.17
7.0	1.09	1.97

Table 4. Characteristics of example spectral types

Spectral Type	T_{eff}	$\log g$	m_V
M0III	3800	+1.34	14.4
G0V	6030	+4.39	19.2
F0V	7200	+4.34	17.4
B5III	15000	+3.49	12.4

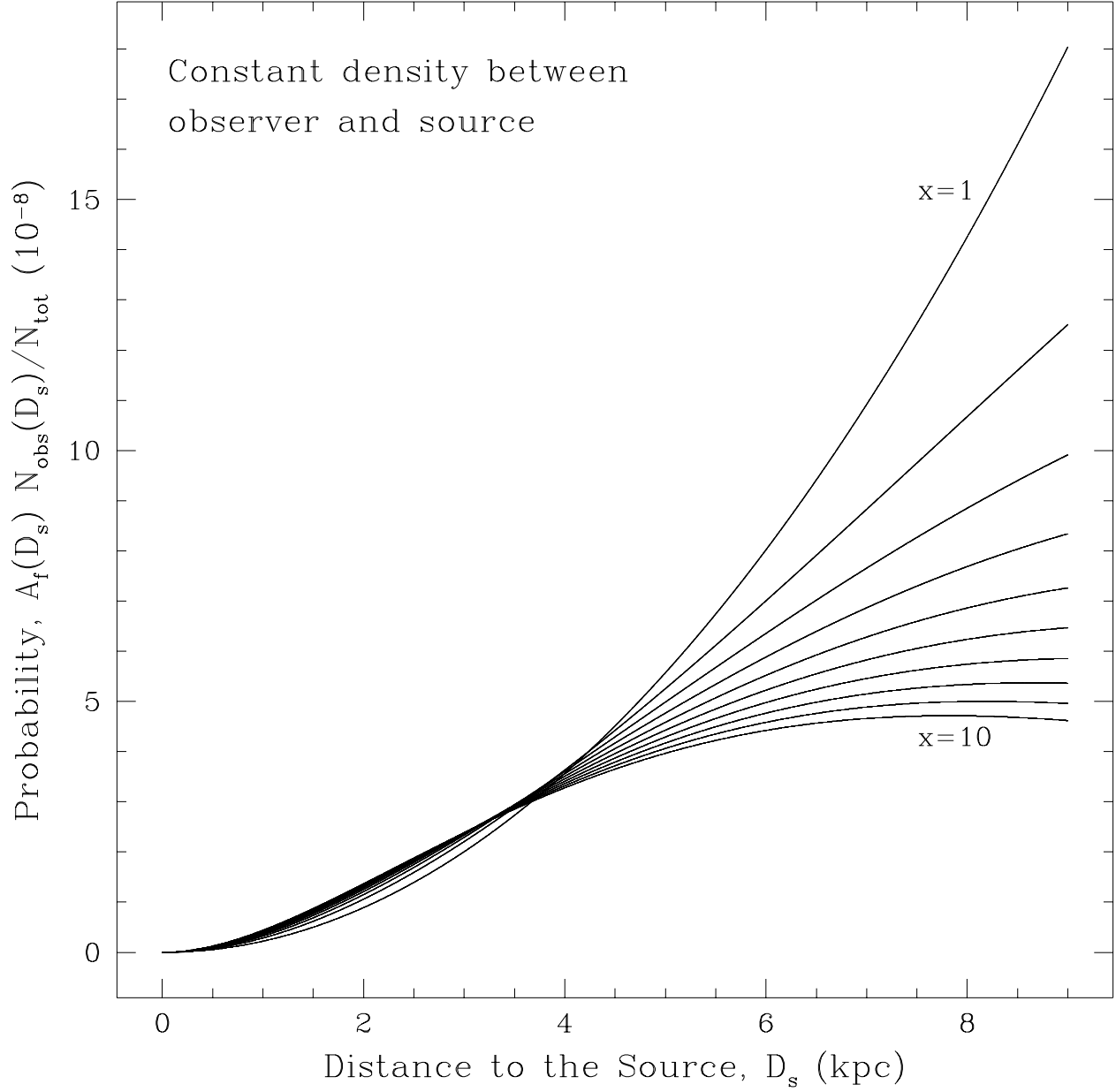


Fig. 1.— Probability as a function of distance to the source for increasing levels of extinction from $x = 1$ (zero extinction) to $x = 10$.

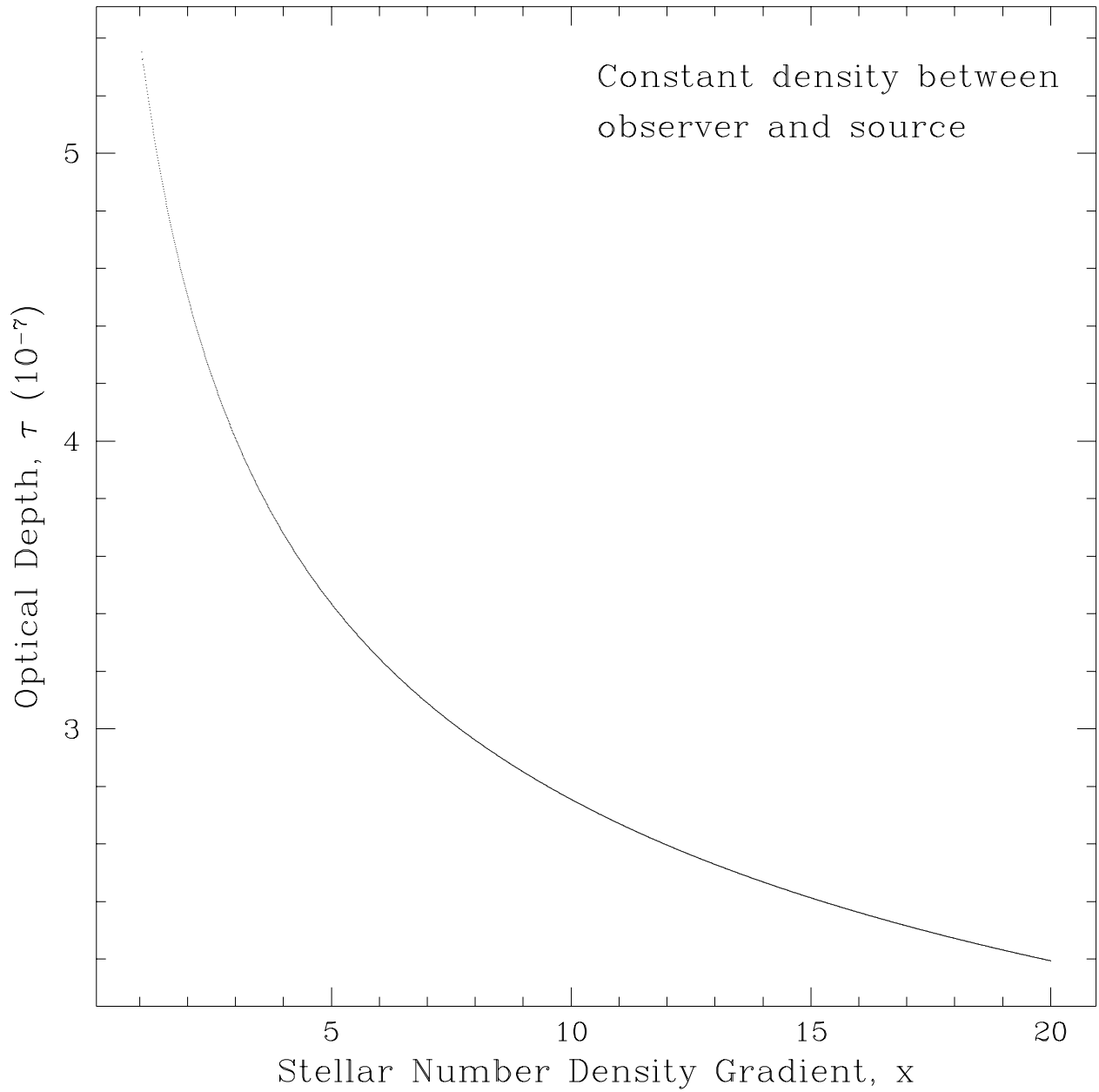


Fig. 2.— Optical depth as a function of the stellar number density gradient x , which is the ratio of observed stellar number density in the nearest and the farthest region in a given line of sight.

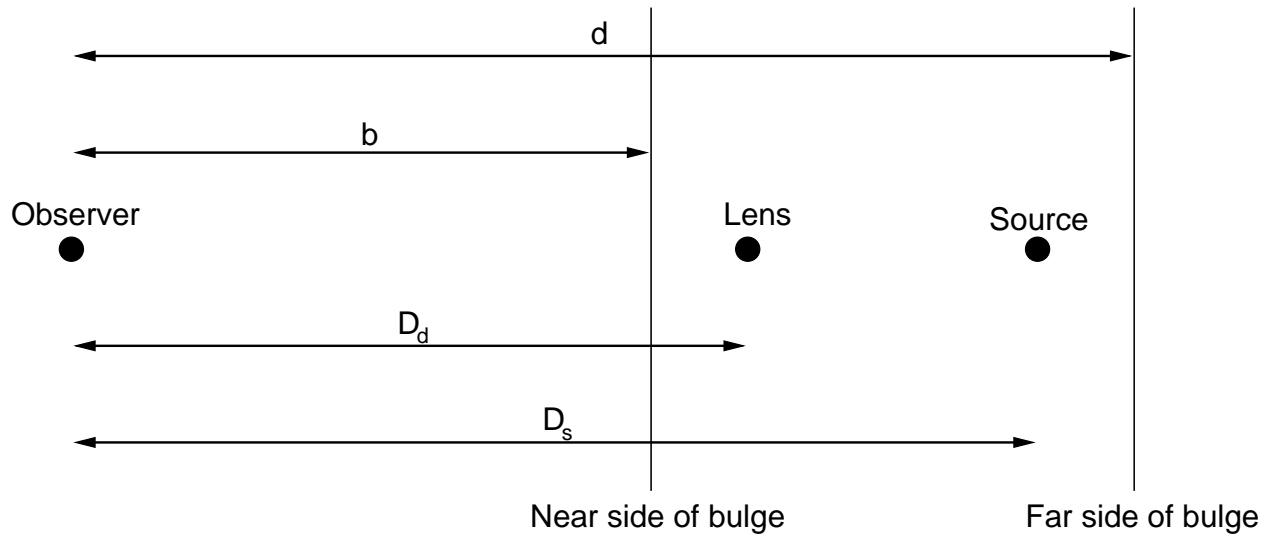


Fig. 3.— Galactic model using a constant density for the disk and a constant density for the bulge. This model assumes that all the microlensed sources are within the bulge.

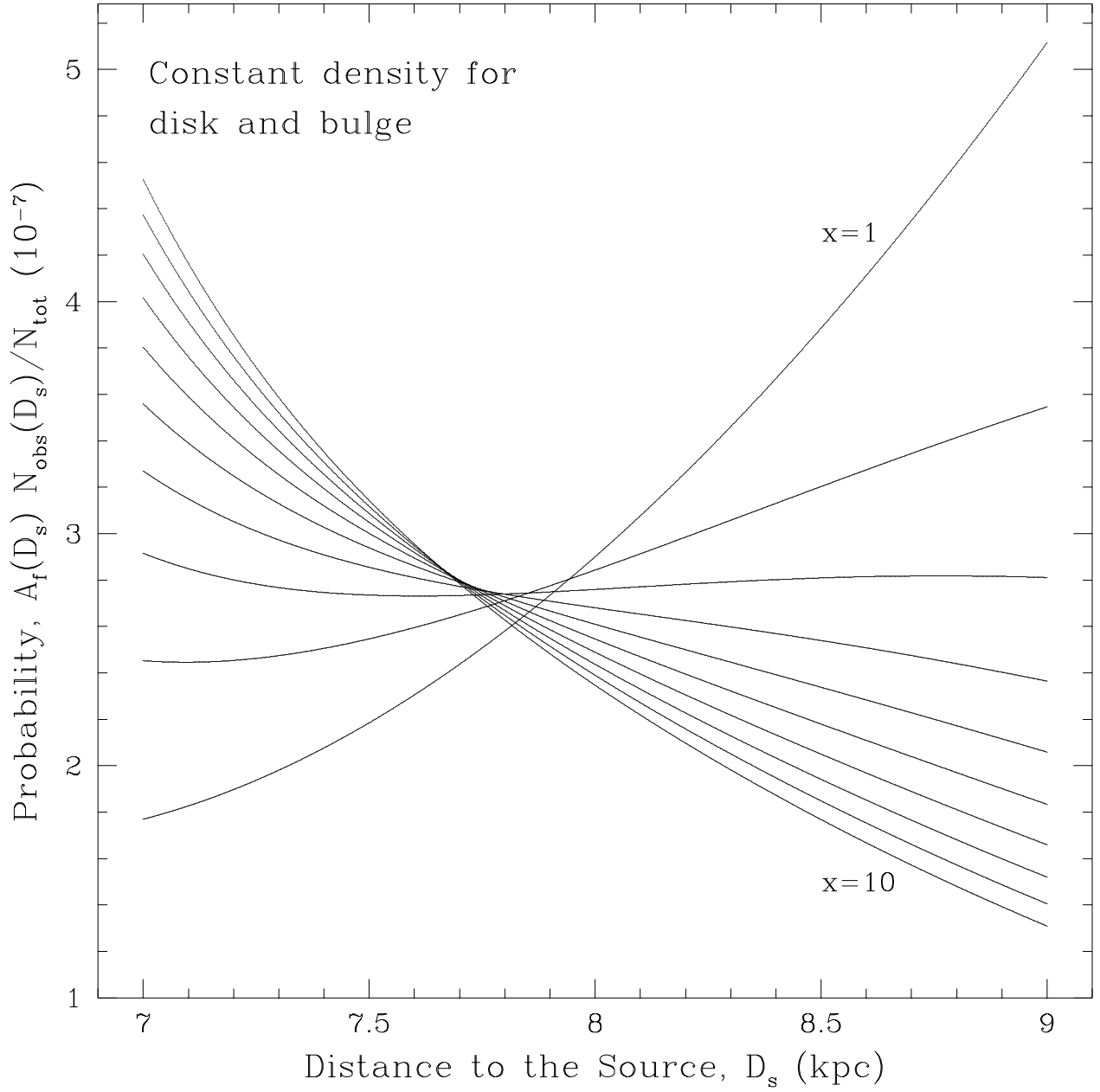


Fig. 4.— Probability as a function of distance to the source for increasing levels of extinction from $x = 1$ (zero extinction) to $x = 10$.

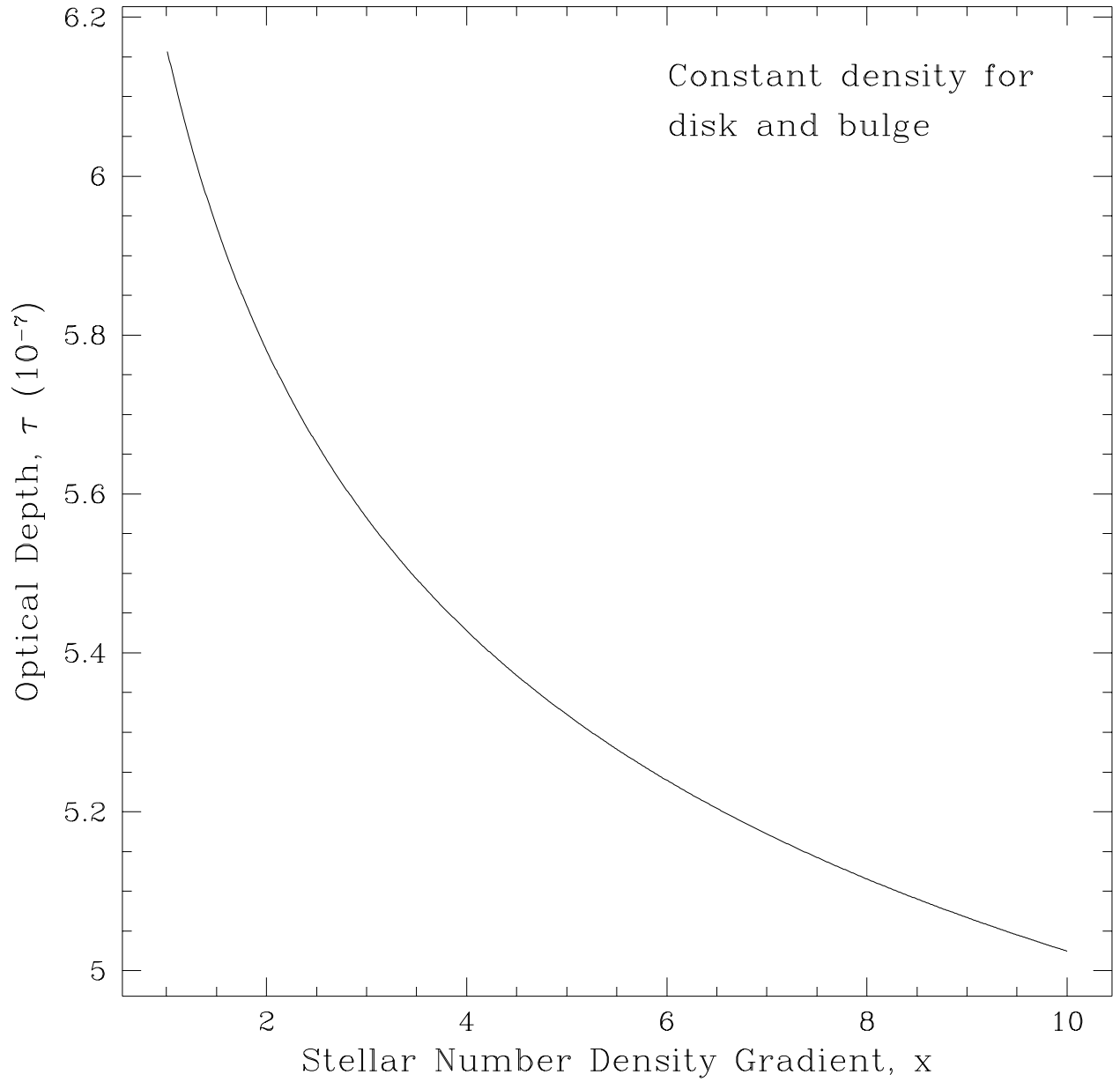


Fig. 5.— Optical depth as a function of the stellar number density gradient x , which is the ratio of the densities of the monitored stars at the near and far sides of the bulge.

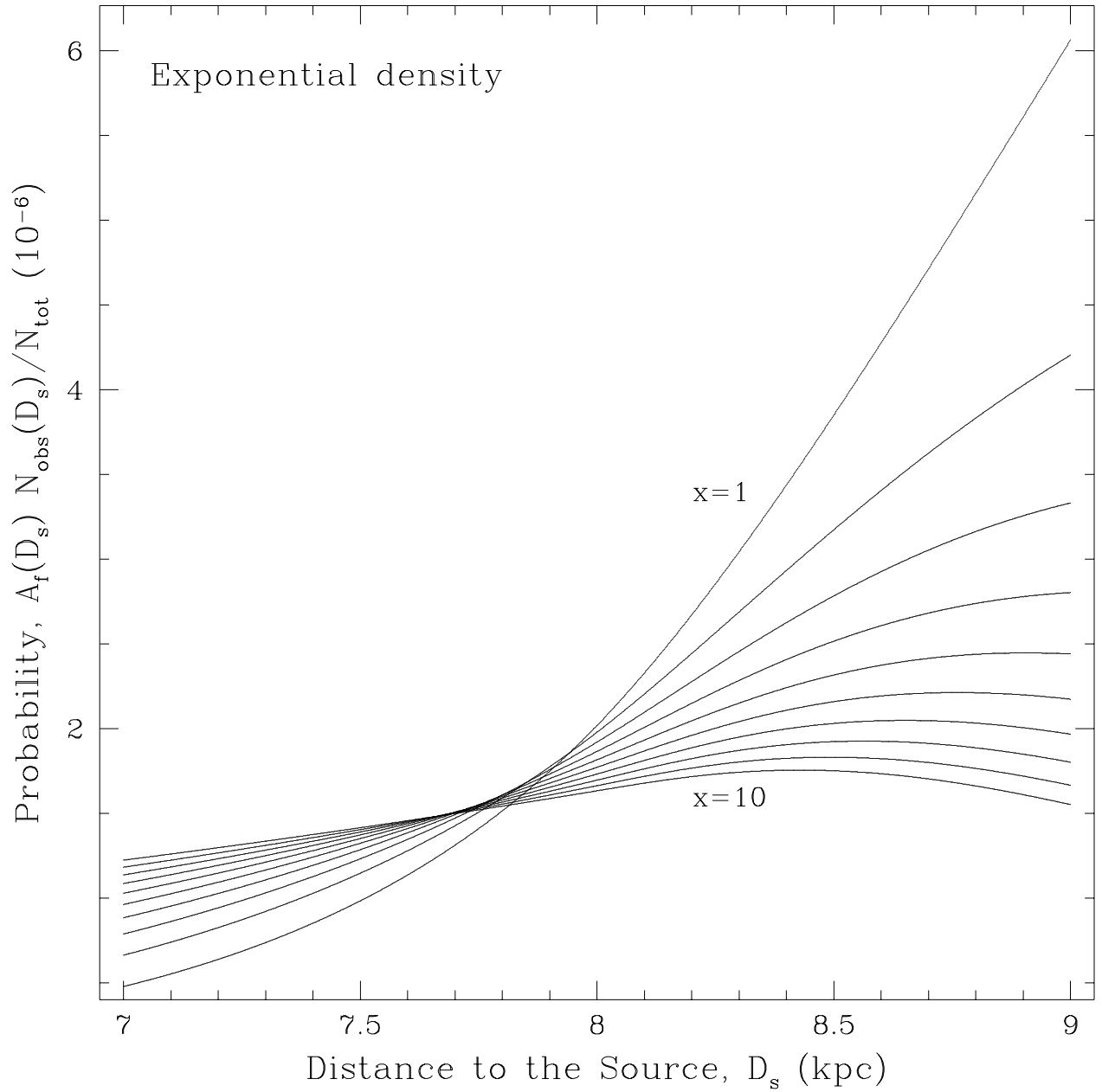


Fig. 6.— Probability as a function of distance to the source for increasing levels of extinction from $x = 1$ (zero extinction) to $x = 10$.

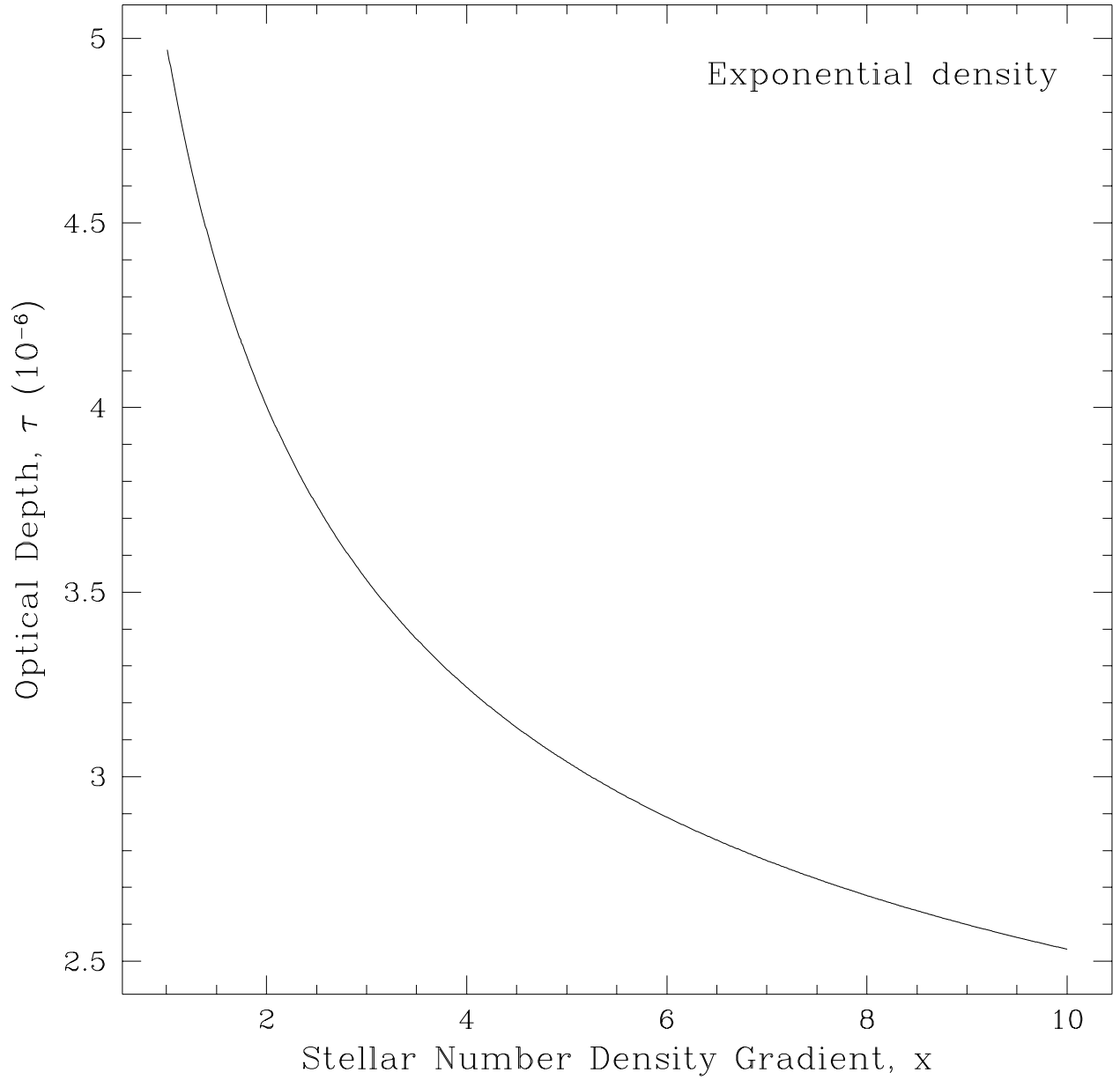


Fig. 7.— Optical depth as a function of the stellar number density gradient x , which is the ratio of the densities of the monitored stars at the near and far sides of the bulge.

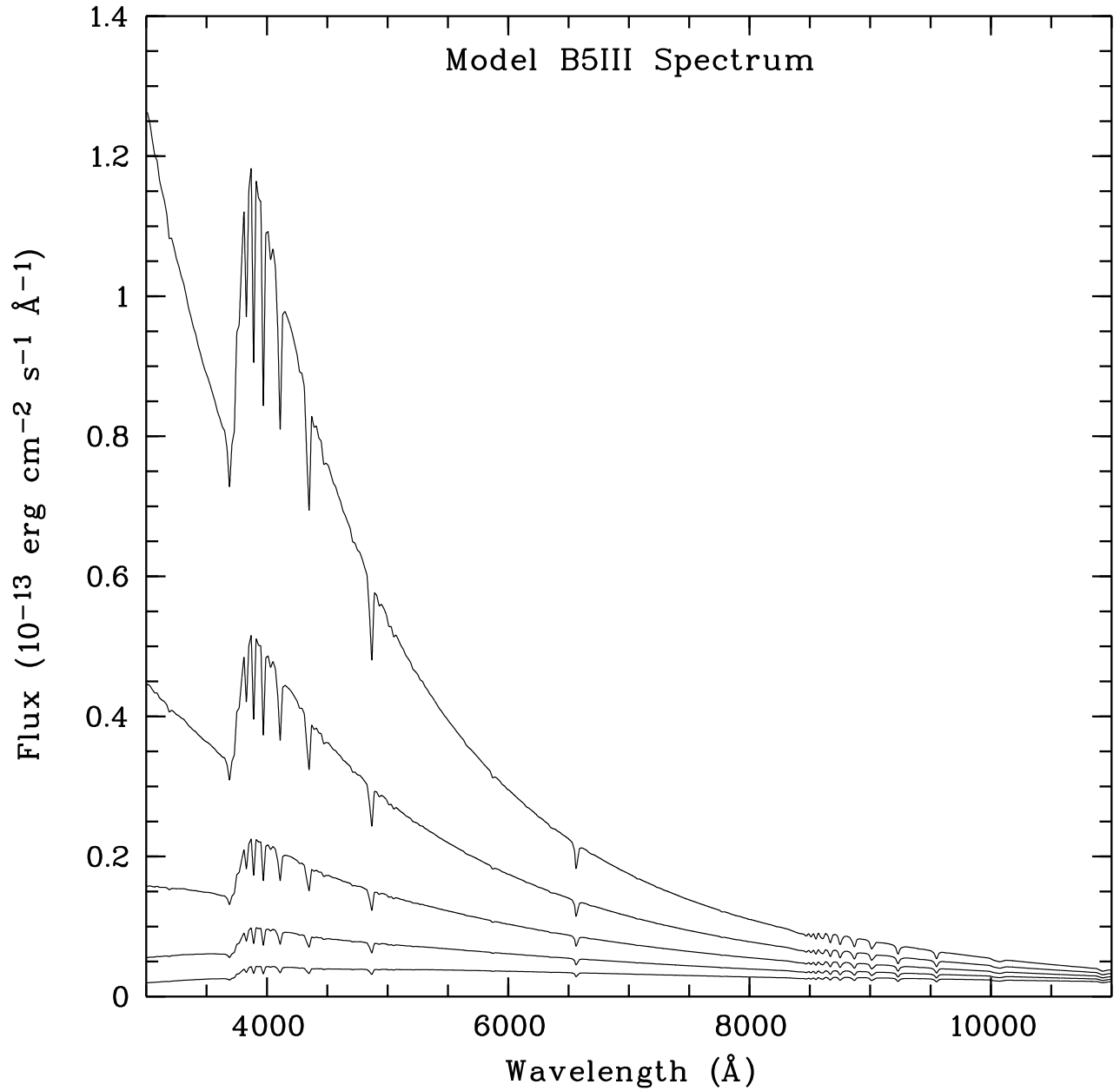


Fig. 8.— Model spectra of a spectral type B5III star showing the effect of increasing levels of extinction from E_{B-V} of 0.0 to 0.8 in steps of 0.2.

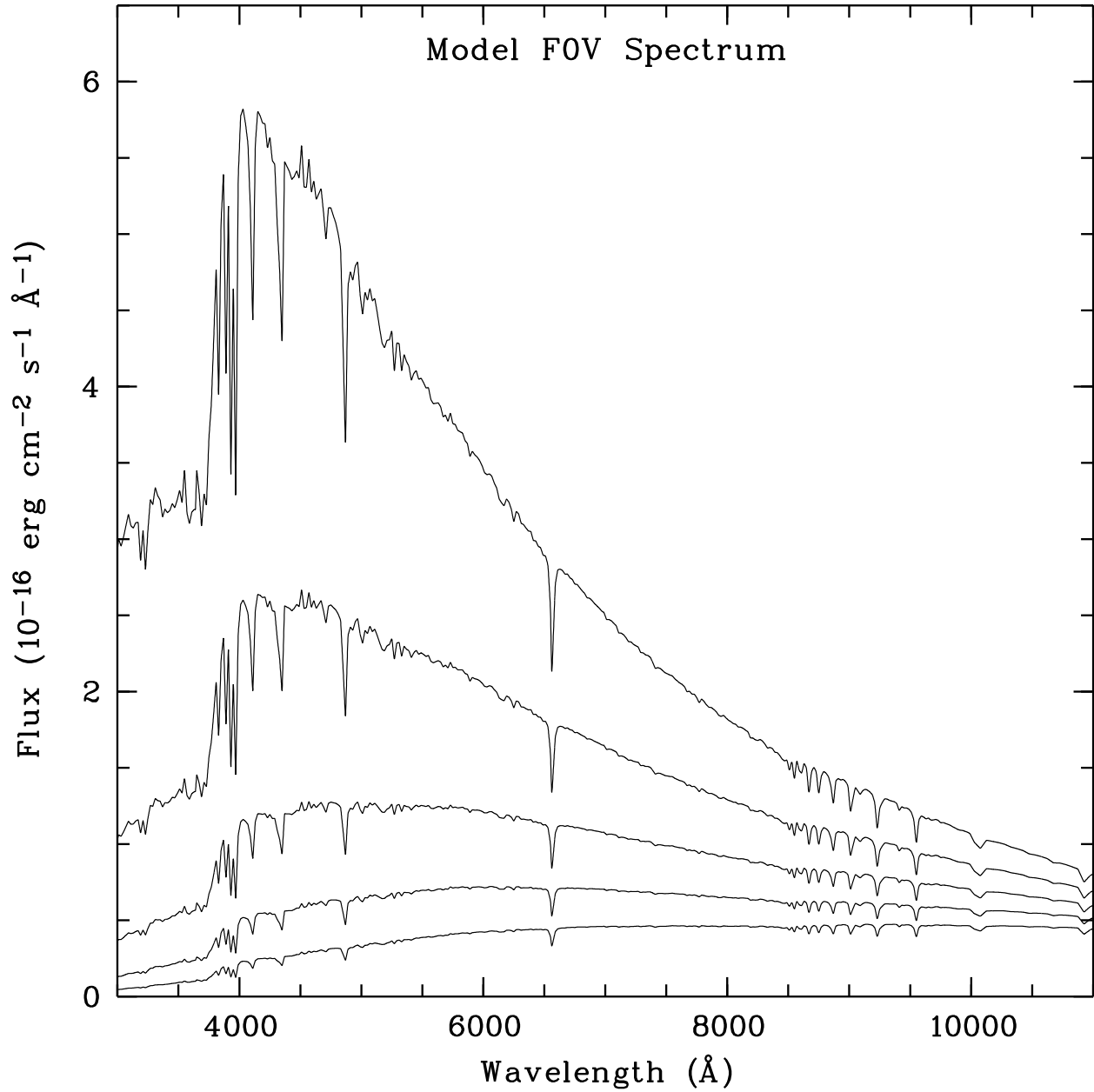


Fig. 9.— Model spectra of a spectral type F0V star showing the effect of increasing levels of extinction from E_{B-V} of 0.0 to 0.8 in steps of 0.2.

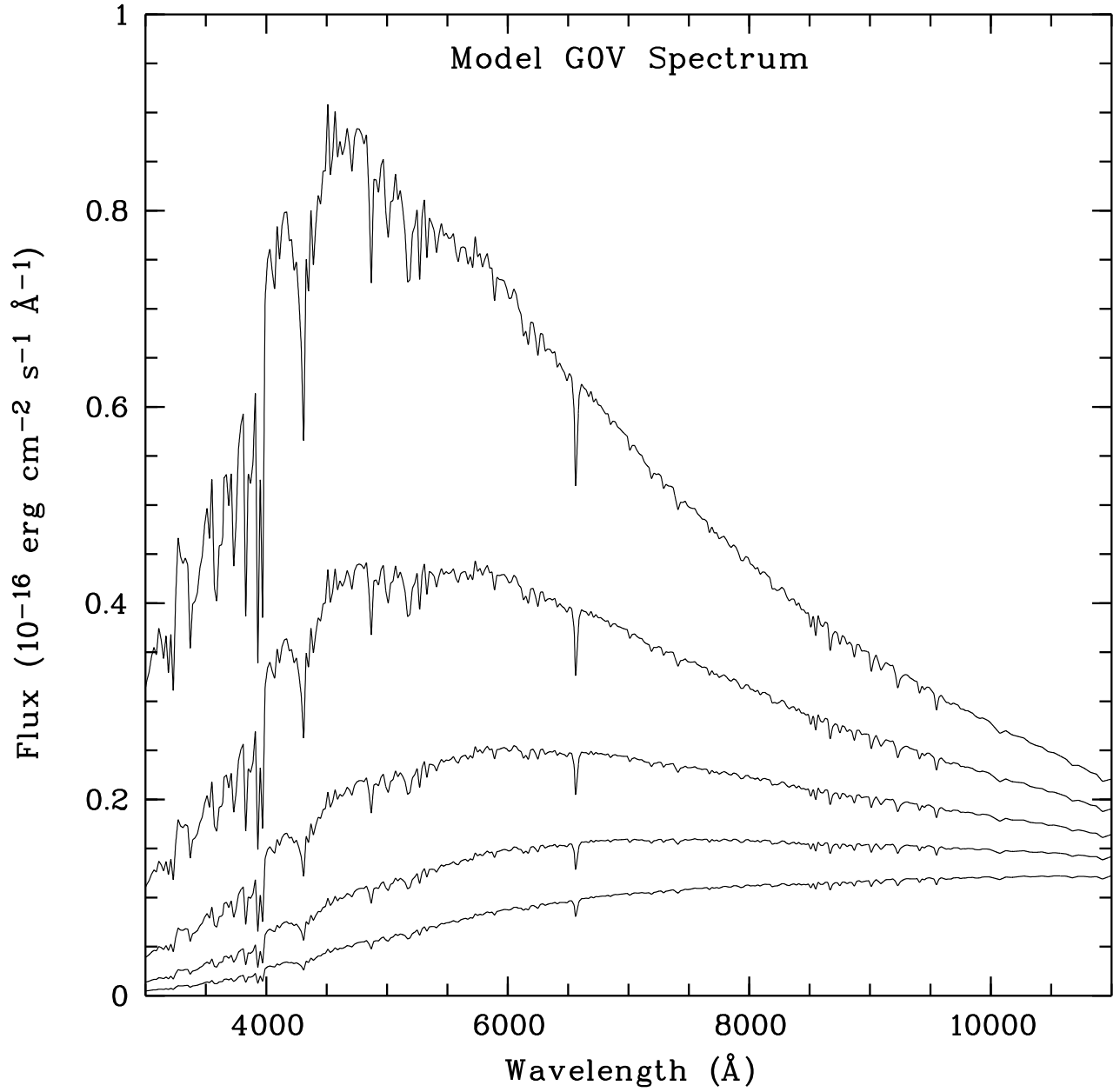


Fig. 10.— Model spectra of a spectral type G0V star showing the effect of increasing levels of extinction from E_{B-V} of 0.0 to 0.8 in steps of 0.2.

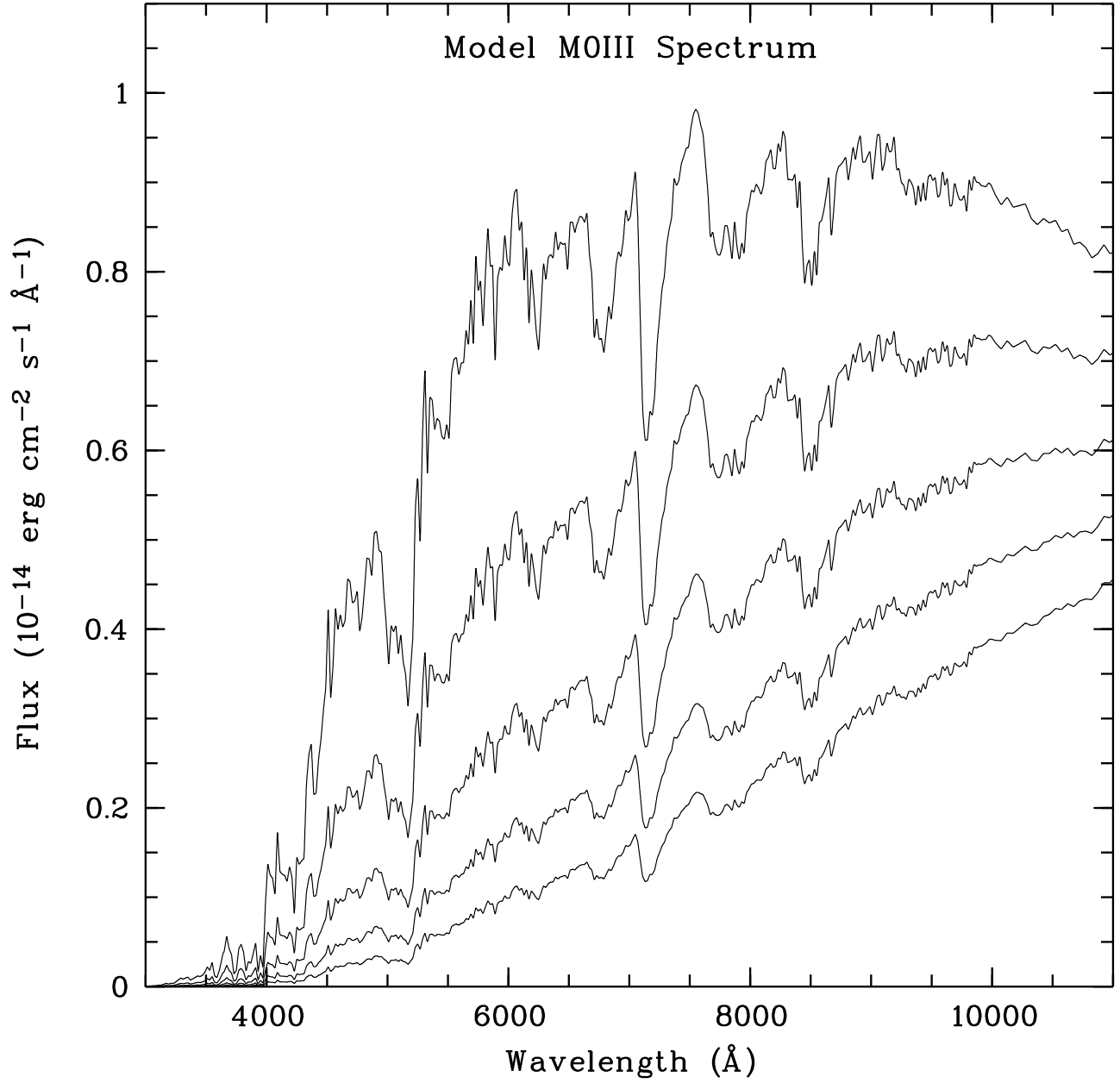


Fig. 11.— Model spectra of a spectral type M0III star showing the effect of increasing levels of extinction from E_{B-V} of 0.0 to 0.8 in steps of 0.2.

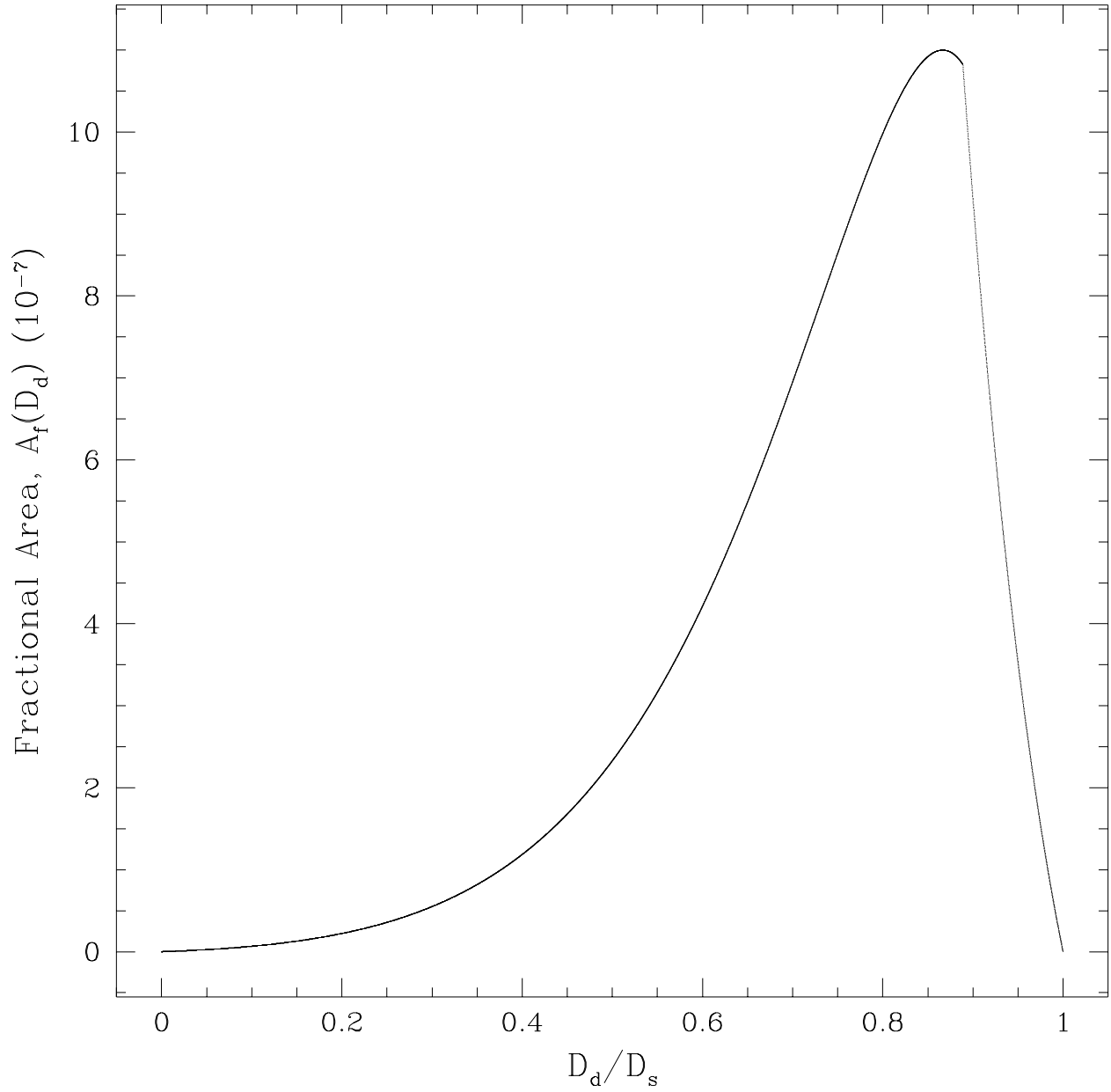


Fig. 12.— A probability distribution for lenses given a source located at a distance of $D_s = 9.0$ kpc. In this case, it is most probable that the lens will be located at a distance of $D_d = 7.8$ kpc.